Supplementing material to report from the hydrogen strategy committee on economy and perspectives. Appendix B

Hybrid fuel cell vehicles
Additional material from LCA analysis
Efficiency considerations

Bent Sørensen
RUC Institute 2, Energy & Environment Group

B.1 The case for hybrid fuel cell vehicles

The possible advantage of using hybrid concepts to speed up the transition to fuel cell vehicles, and possibly as a lasting optimal solution, was mentioned in the main report. Here, a vehicle performance simulation study is presented in support of this view (1[¤]).

In parallel with actual tests on the road, simulations are used by both scientists and auto manufacturers as a means of getting a first orientation at low cost, both before a new car is actually constructed and also during the testing and revision phases. The brief simulation study presented here illustrates the capability of such simplified, but fairly realistic model assumptions.

It is possible to simulate the behaviour of various vehicle types with conventional propulsion systems such as Otto or Diesel engines, pure electric or pure fuel cell vehicles as well as hybrids, either by a detailed physical modelling or by a semi-empirical method, where different processes are simply parametrised and the parameters are adapted to measured data. The latter method is presented here, based on the software ADVISOR developed for the US government by NREL in Golden, CO. Parametrised models exist for fuel cell stacks, electric motor, battery energy storage, power-train control in fuel cell cars with battery, exhaust control, power behaviour of the wheel/axle system under prescribed driving conditions (slope, road surface and resistance, etc.) and also auxiliary electric energy use in the vehicle. The actual programme uses the required driving speed at a given time to calculate torque, rotational speed and power in each drive-train element, a procedure called a backward-facing simulation approach. However, this is combined with a forward-facing approach based on the control logic, and the simulation proceeds forward in time, but with backward consistency checks at each step.

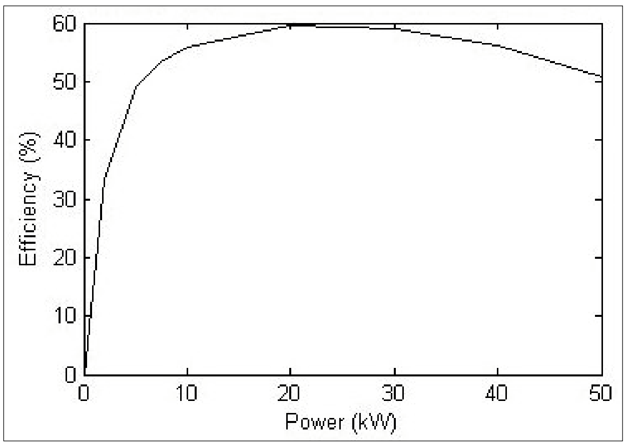

Figure A2.1. Power curve for the 50-kW PEM fuel cell used in simulations.

[¤] References refer to the list at the end of the main report.

The fuel cell modelling is either a simple one where power output and efficiency are linked by an empirical curve such as the one shown in Figure A2.1, or a combination of relationships for each component in the fuel cell system. For the simulations reported below, the two methods gave similar results. More detailed models, e.g. treating water management, are available in the literature. For the battery, additional calculations were made with the battery assumed unable to be recharged by the fuel cell, as well as with batteries in various hybrid configurations. Both conventional lead-acid and advanced lithium ion batteries have been modelled, using internal resistance battery models.

The fuel cell vehicle considered is an artefact loosely modelled over the Volkswagen Lupo TDI-3L (see section 3.4 of main report), so for simplicity, I shall call it *Little Red Ridinghood*. The 45-kW diesel engine is replaced by a fuel cell engine in a hybrid configuration with battery power, ranging from pure fuel cell operation to a pure electric vehicle. Suitable component rating is determined on the basis of efficiency for a given driving cycle rather than (poorly known) cost, sometimes leading to several systems of comparable performance. The total mass of the each *Little Red Ridinghood* configuration has the distribution shown in the table below (compare to Table 1 in section 3.4 of the main report, for the Diesel Lupo 3L).

Component mass (kg)	***pure FC***	***hybrid***	***pure EV***
Basic vehicle (incl. start battery)	604	604	604
Fuel cell equipment (30, 20 and 0 kW)	163	133	0
Exhaust management	8	5	0
Lithium ion batteries (2-3 times more for Pb)	0	113	681
Electric motor	44	58	70
Transmission (manual 1-speed equivalent)	50	50	50
Passengers and cargo (average)	136	136	136
Total	**1005**	**986**	**1541**

Table. Mass distribution for Little Red Ridinghood fuel cell-electric hybrid vehicles.

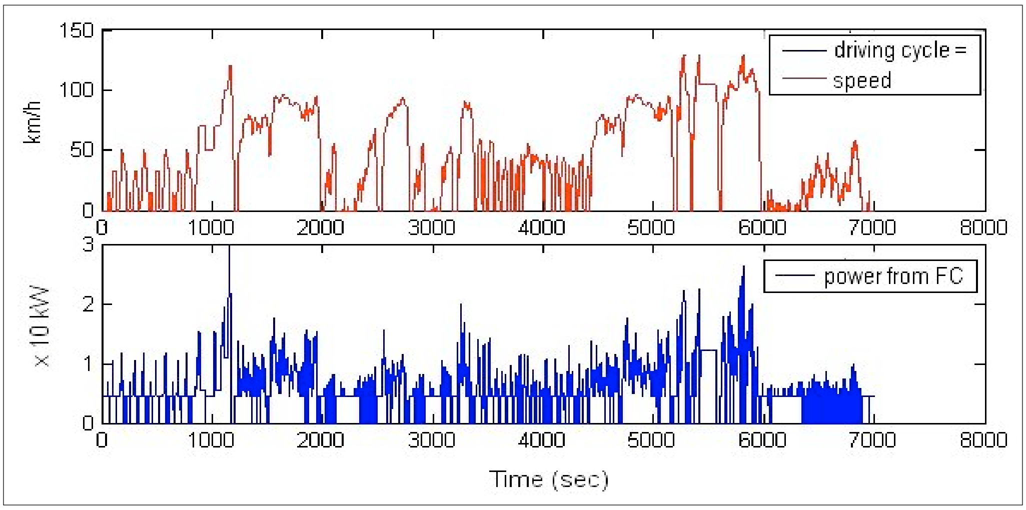

Figure A2.2. Simulation results for the *Little Red Ridinghood* pure 30-kW fuel cell vehicle under a mixed driving cycle (matching achieved speed). Equivalent gasoline fuel use is 2.7 litre per 100 km. See text for further discussion (1).

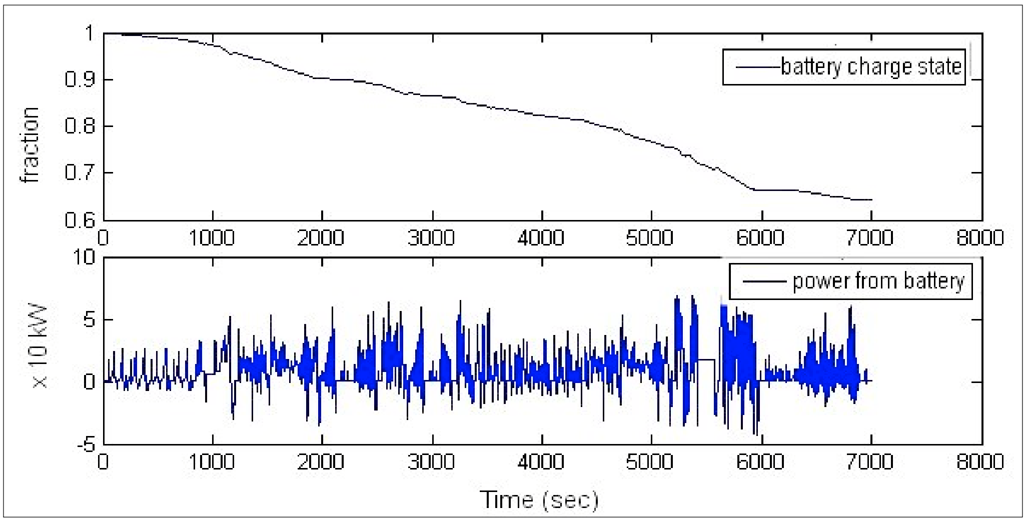

Figure A2.3. Simulation results for *Little Red Ridinghood* in a pure electric vehicle version with 1650 kg lead-acid batteries. The equivalent gasoline fuel use is 2.7 litre per 100 km, and 2.5 and 1.7 l/100 km for corresponding simulations using nickel metal hydride and lithium ion batteries (1).

As the driving cycle used in the simulations, an 89 km sequence of city and highway standard cycles has been used. This driving cycle, which is shown at the top of Figure A2.2, comprise the New European Driving Cycle (at the beginning) and the US Urban Dynamometer Driving Schedule (UDDS) from 3100 to 4400 sec. The cycle does not include slopes, but has more frequent decelerations and accelerations during the highway parts, making it as demanding as a graded path.

Figure A2.2 shows the simulation results for a pure fuel cell car. The driving cycle-prescribed speeds at top are also the achieved speeds. The second graph shows the power delivery from the fuel cell to the electric motor, peaking at 30 kW at the moments of maximum acceleration. The rated fuel cell power is taken as 30 kW, which is sufficient for all periods of the driving cycle used. Actually, lowering the rated power to 20 kW makes so little difference in respect to achieved speed, that it is not visible on a similar graph. However, the fuel cell is then working much of the time at high power levels, and any smaller fuel cell ratings do not allow the driving cycle speeds to be reached at all times. The fuel consumption is 76 MJ of hydrogen for the 89-km cycle, corresponding to an equivalent gasoline fuel economy of 2.7 l/100 km (2.3 l/100 km for the 20 kW simulation). In order to have a range of 600 km, the car must then carry 4 kg of hydrogen. This agrees well with the 1.8 kg carried in two modest size compressed gas containers by the prototype Daimler-Chrysler f-cell car (cf. Table 1 in main text) for a range of only 150 km and with a prototype Ballard fuel cell of lower than the goal efficiency expected to be reached within a few years. The 4 kg hydrogen would have a volume of 178 litres at 30 MPa.

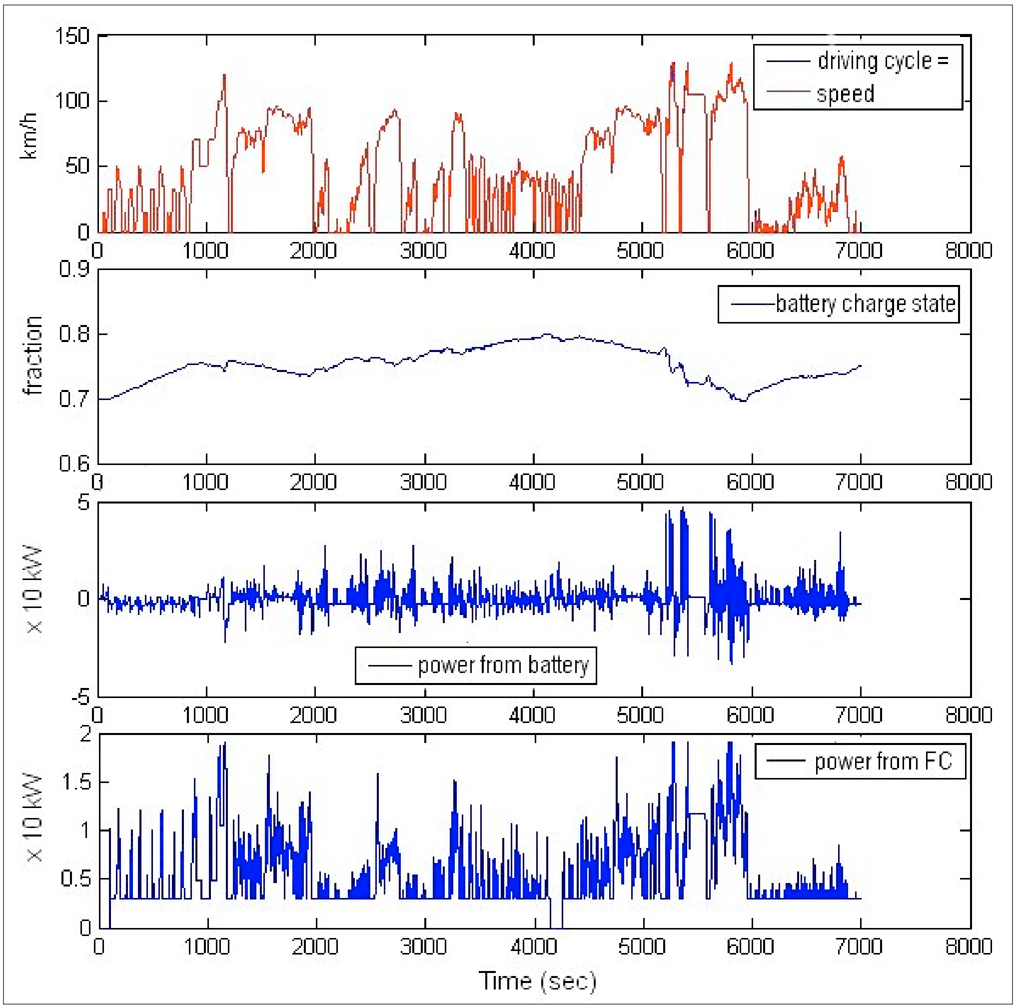

Figure A2.4. Simulation results for the Little Red Ridinghood fuel cell-electric hybrid vehicle with 20 kW of fuel cells and 113 kg of Li ion batteries. Equivalent gasoline fuel use is 2.4 litre per 100 km. See text for further discussion (1).

Figure A2.3 shows the simulation results for a pure electric vehicle built upon the same concept. Three versions have been modelled, using lead-acid, nickel metal hydride or lithium ion battery technologies, and Figure A2.3 shows the results for a 17-kWh Pb battery, adding 1650 kg of mass to the vehicle and yet achieving a range of no more than 250 km. With a 17-kWh NiMH battery, the range is increased to 350 km, with a battery mass of 1670 kg. The problem with pure battery operation is that adding battery capacity strongly influences total weight and thus creates a further need for traction power in a vicious circle. If, alternatively, the recently developed large lithium ion-type batteries are introduced, the additional mass can be kept down to 680 kg, with a range of 300 km and 12.3 kWh of stored energy, for the different characteristics of Li ion batteries (7). The fractional discharge state and the actual power output of the batteries are nearly identical for the three simulation runs, of which the Pb battery results are used in Figure A2.3. The maximum discharge rate of the batteries is near 70 kW. This is very different from the 30 kW for the pure fuel cell power system, because of the different discharge characteristics of batteries.

Finally, Figure A2.4 shows the simulation results for a hybrid fuel cell-electric vehicle with 20 kW of fuel cells and a 5-kWh, 113 kg Li ion battery. The two power sources are operating in series, and particularly during the high-speed highway part of the driving cycle (at 5000-6000 sec), both contributes to propulsion, peaking at 19 and 47 kW but with simultaneous power limited to 58 kW by the motor. The fuel cells have surplus power to charge the batteries during periods of low power requirement (the low-speed segments of the driving cycle), but exhibit a net discharge during high-speed segments. The charge state of the battery at the end of the 89-km cycle is slightly higher than at the beginning (as it should be because the final speeds are low).

Lower than 20 kW fuel cell rating leads to insufficient battery charging. Increasing the fuel cells to 30 kW, with a lowering of the Li ion battery size to 3 kWh (mass 69 kg), gives an overall performance similar to that of Fig. 4.8 (but of course with larger variations in battery charge state). In fact, even with a 1 kWh battery, the 30 kW fuel cell can handle the demands of the driving cycle, so there is no clear optimum configuration, but a range of technical options depending on e.g. requirements to performance in extreme situations not covered by the selected driving cycles.

An electric motor of efficiency 0.92 and a manual 1-speed transmission have been used for all the simulations. The transmission often constitutes a significant loss factor, and losses in using 5-speed or automatic transmissions are higher than for the 1-speed gearbox. Because the actual Lupo 3L has an electronically operated automatic transmission with higher efficiency than the corresponding manual transmission, the 1-speed model was selected in order to avoid a distorting impact on the simulation results.

The simulation study indicates the advantage of using fuel cells in a hybrid configuration together with a modest size advanced battery, in order to achieve a range not achievable with battery-only vehicles, and with a fuel cell rating much lower than for a pure fuel cell vehicle. The result is a lowering of cost relative to either pure battery or pure fuel cell vehicles with similar performance (if possible). A transition technology towards the fuel cell hybrid vehicle is the gasoline- or diesel-battery hybrid available today (e.g. Toyota Prius). It would appear a good idea to arrange Danish vehicle taxation that does not disfavour increasing use of such solutions both in the short-term and in the longer term.

B.2 Additional material from LCA analysis

Figure A2.5 gives the environmental LCA data available for these cars, in terms of energy used and emissions occurring during the phases of the vehicle life-cycle, based on (1, 36). The impacts are given in physical units as required for the LCA inventory and are subsequently translated into concrete impacts on health and environment, including global warming effects. The impacts from the manufacture and use of the fuel cell component in the *f-cell* car are further discussed in (1). The fuel cell vehicle considered in this study use hydrogen directly. If reformation of methanol or gasoline were used, additional impacts would derive from the reformer, including often quite large impacts from catalyst such as palladium, which again should be recycled as fully as possible.

No separate data have been found for decommissioning impacts, although VW claims to have included them under “lifetime operation” (34). In Denmark, cars delivered to a recycling station pay a fee of about 500 euro, assumed to cover the decommissioning costs minus income from selling extracted parts for reuse. European regulation is discussed, where decommissioning is part of the initial purchase price and the manufacturer is obliged to optimise assembly for decommissioning and to take the vehicle back at the end of service for maximum recycling.

The Volkswagen report is a detailed and site-specific LCA for the manufacturing plant at Wolfsburg including materials and water delivered to or coming out of the plant. It is centred on the Golf cars, but the scaling for application to Lupo made here has in gross terms already been made in the VW environmental report (34). Numerical values can be found in tables given in (1, 36).

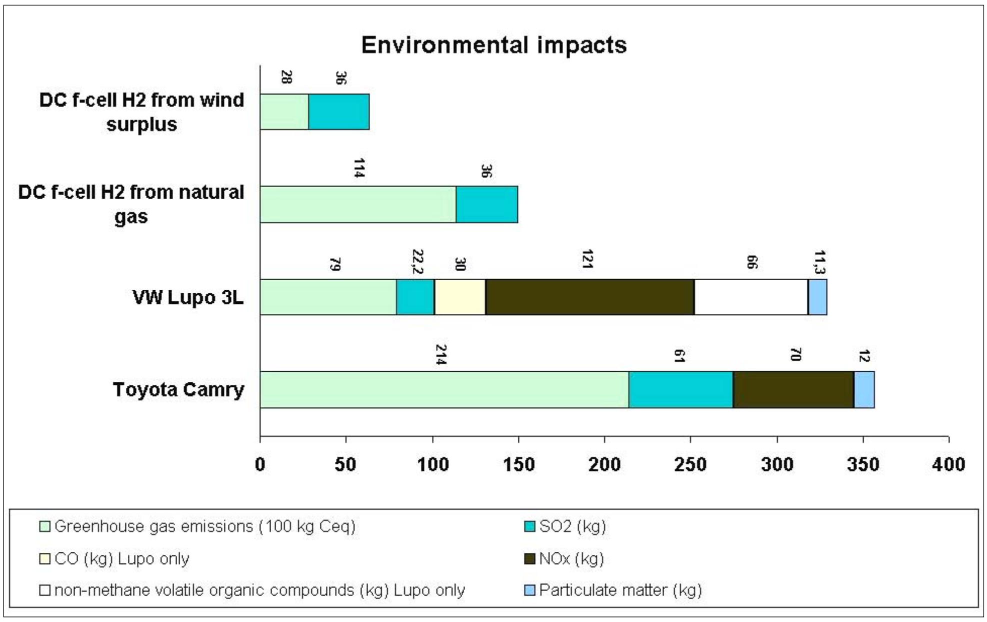

Figure A2.5. Comparison of environmental impacts from the three passenger vehicles considered in the life-cycle analysis (assumed 15 year, 300 000 km driven), with hydrogen for the fuel cell car being derived from either natural gas or excess wind power (1).

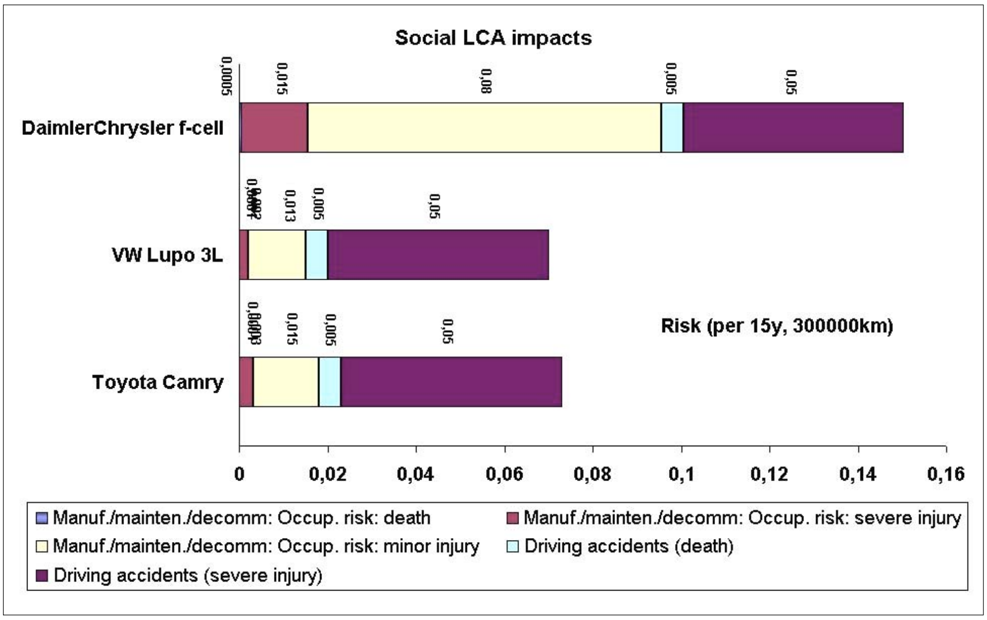

Figure A2.6. Comparison of social impacts from the three passenger vehicles considered in the life-cycle analysis (1).

Figure A2.6 gives occupational risks during the life cycles of the vehicles, based on standard industrial data (i.e. the impacts are proportional to cost). The job content is based on statistics from the energy sector in Denmark (30). The rate of accidents on the road are taken from several Danish studies and is considerably higher in some parts of the world. Evaluation of the health and injury impacts are again based on several Danish studies (references (30)), as are the less tangible visual and noise impacts (estimated by hedonic pricing), and the inconveniences such as children having to be supervised when near public roads, or pedestrians in general having to use round-abouts to get to street crossings with traffic lights, where also the waiting time is valued.

B.3 Efficiency considerations

One criticism sometimes launched against the hydrogen infrastructure system is that the many conversion steps involved will make the overall efficiency of the system low (65). From wind electricity through electrolysers to hydrogen, with transportation and storage losses, to finally regenerate electricity in buildings or fuel cell vehicles entails an overall efficiency of around 25%, which is seen as low compared with the present efficiency. The latter is between 13% and 30%, considering refinery losses (10%) and either vehicle combustion engines (average efficiency about 15%) or power plants (average efficiency at or below 35%). According to (1), the criticism is ill placed, because the whole point is that the present fossil fuel system is drawing near its end and has to be replaced by another energy system. Since renewable energy offers the only sustainable future energy system, the handling of variable primary energy streams is a must. Handling such fluctuations requires storage of energy, and hydrogen seems to be the cheapest way of accomplishing this. Clearly converting back and forth involves additional losses, but that cannot be helped, and a fair comparison of hydrogen systems would be with other systems capable of handling the large fluctuations of solar and wind energy, not with the obsolete system on its way out. Such a fair comparison will most likely designate hydrogen as the most viable energy storage medium, with underground hydrogen storage as very attractive compared with batteries, pumped hydro and other storage possibilities.

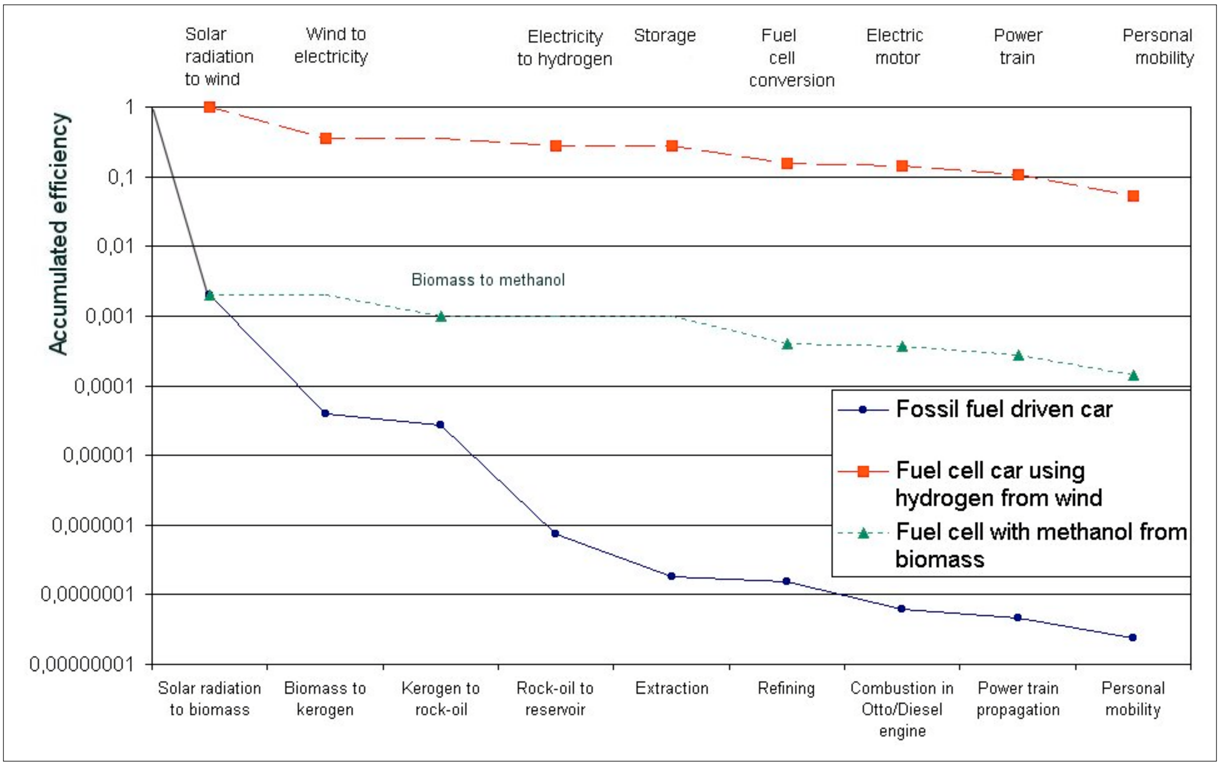

Figure A2.7. Stepwise accumulated efficiency of chains of energy conversion from primary sources to end-use, taken here as personal transportation. Current vehicles based on oil products are compared to fuel cell vehicles using methanol from biomass or hydrogen from wind (1). See text for details.

The criticism against fuel cells and hydrogen going through stores has widely discussed, e.g. in (8). The claim made by the critics, that the efficiency of hydrogen systems is low when all stages of conversion is included in the considerations, may be rebutted by noting that use of variable renewable energy sources in any case must involve some part of the system's energy going from the form of electricity through stores based on other energy forms and subsequently back to electricity, with the associated unavoidable losses. In order to put this argument in perspective, Figures A2.7 and A2.8 show the accumulated efficiencies through all conversion stages (assuming based on the renewable energy scenarios in Chapter 5 of (1) that 50% of the power used outside the transportation sector has to be regenerated from hydrogen stored). For comparison, the similar efficiency chains are shown for oil and coal used in the current energy system. The calculation involves the following steps:

First, Figure A2.7 considers for fossil and biomass routes the production of biomass from solar radiation, at an average efficiency of 0.2% (7). For the petroleum products, the efficiency of the (million year) fossilisation processes of kerogen formation (2%), oil formation in rocks (67%, the rest being natural gas, of which some escapes) and flow into exploitable reservoirs (2.8%) are taken from (9). Average extraction efficiencies are estimated as 24.5% and refinery losses as 15%. The combustion efficiency in vehicle Otto or Diesel engines is about 40%, power train efficiency 75% and the end-use benefits of overcoming air resistance and friction or elevation losses 50% (Chapter 6 in (1)). The overall accumulated fossil-fuel car efficiency is thus as low as 2.3 $\times 10^{-8}$. For the methanol route the solar-to-biomass efficiency of 0.2% is followed by a methanol production efficiency (50%), a DMFC or reformer-PEMFC efficiency of 40%, an electric motor efficiency of 93% and the same power train and driving efficiencies as for the fossil fuel car. Finally, for the hydrogen fuel cell car, the solar radiation to wind conversion efficiency is taken as 100% (following arguments from (19)), the wind turbine efficiency as 35%, the electrolysis efficiency as 80%, the fuel cell conversion efficiency as 55% and the rest as for methanol. The overall accumulated efficiencies are 1.4×10^{-4} for the methanol route and 0.054 for the wind-hydrogen route.

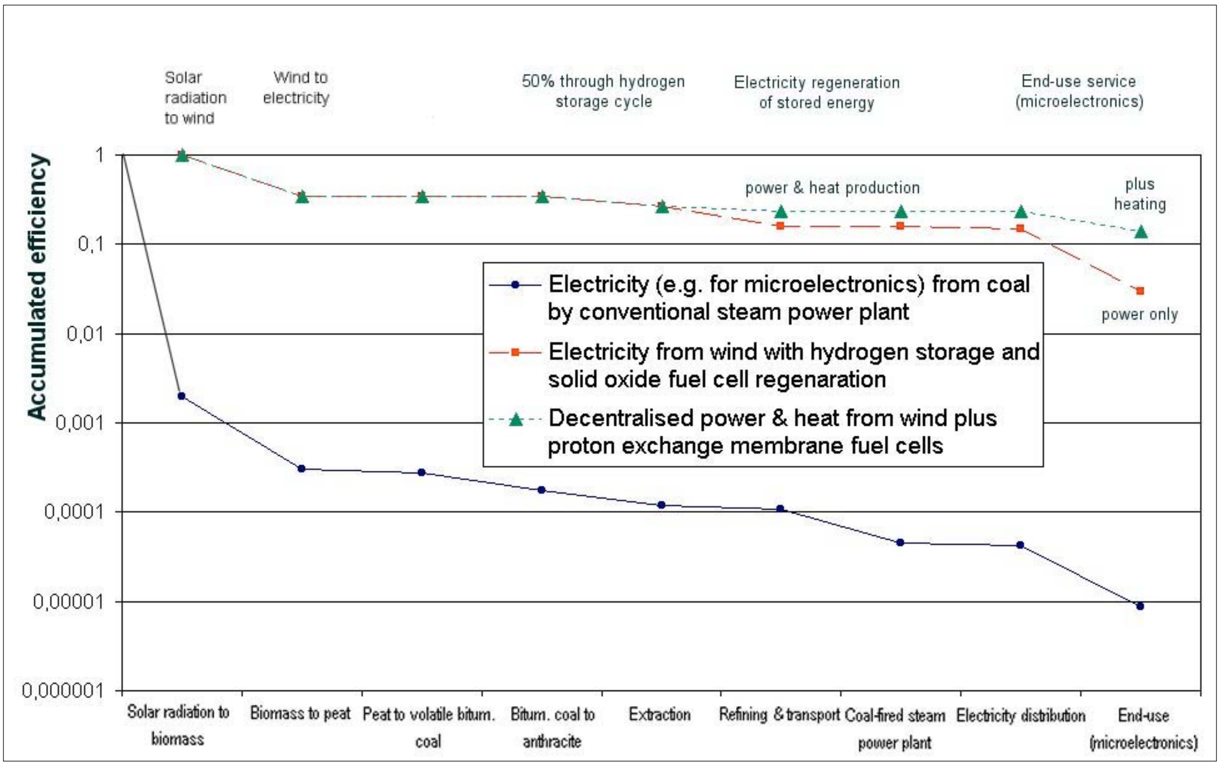

Figure A2.7. Stepwise accumulated efficiency of chains of energy conversion from primary sources to end-use, taken here as the operation of electronic equipment by electricity. Current electricity production based on coal is compared to renewable electricity from wind, of which some go through hydrogen stores and are converted back to electricity with and without utilisation of associated heat (1). See text for details.

In Figure A2.7, following the solar energy to biomass efficiency (0.2%), the successive transformation into peat, highly volatile bituminous coal and finally hard coal (anthracite) carries efficiencies of 15%, 92.5% and 63% (9). A typical efficiency of coal extraction (average of surface and deep mining) is 69%, that of refining and transport 90%. The steam power plant efficiency is taken as 42%, the electricity transmission and distribution efficiency as 94%. Finally, an average to high-end end-user efficiency of using electricity (say in a microelectronic device) is 20%. The first steps of the renewable routes is as above (35% wind turbine), but as under half of the power is assumed to be used directly and the remaining going through a hydrogen store (cf. Chapter 5 of (1)), an average storage cycle efficiency of 75% is assumed, covering electrolysis and hydrogen storage/transmission losses, but not electricity regeneration which is assumed to be 60% for the centralised SOFC route and 50% electric plus 40% heat efficiency for the decentralised PEM route. In the centralised case, a transmission and distribution loss of 6% is subtracted, while for the decentralised case, the in-house losses are confined to 1%. The electricity to microelectronic device performance efficiency is still taken as 20%, but a 40% waste heat in-house use is added in the decentralised case.

In this perspective, the renewable energy, hydrogen store and fuel cell routes are much more efficient than the current systems.